AD-A035 605 NAVAL RESEARCH LAB WASHINGTON D C F/G 20/4
DYNAMIC STABILIZATION OF THE RAYLEIGH-TAYLOR INSTABILITY ON LAS--ETC(U)
DEC 76 J P BORIS
UNCLASSIFIED NRL-MR-3427 NL

1 OF 1
ADA035605

END

DATE
FILMED
3-77

12

NRL Memorandum Report 3427

Dynamic Stabilization of the Rayleigh-Taylor Instability on Laser-Imploded Shells

JAY P. BORIS

Plasma Dynamics Branch
Plasma Physics Division

December 1976

This Work was sponsored by the Office of Naval Research
Under Contract RR011-09-41

NAVAL RESEARCH LABORATORY
Washington, D.C.

SECURITY CLASSIFICATION OF THIS PAGE (When Data Entered)

REPORT DOCUMENTATION PAGE	READ INSTRUCTIONS BEFORE COMPLETING FORM
1. REPORT NUMBER: NRL Memorandum Report 3427	2. GOVT ACCESSION NO. / 3. RECIPIENT'S CATALOG NUMBER: NRL-MR-3427
4. TITLE (and Subtitle): DYNAMIC STABILIZATION OF THE RAYLEIGH-TAYLOR INSTABILITY ON LASER-IMPLODED SHELLS.	5. TYPE OF REPORT & PERIOD COVERED: Interim report on a continuing NRL problem.
	6. PERFORMING ORG. REPORT NUMBER
7. AUTHOR(s): J. P. Boris	8. CONTRACT OR GRANT NUMBER(s): RR0110941
9. PERFORMING ORGANIZATION NAME AND ADDRESS: Naval Research Laboratory, Washington, D.C. 20375	10. PROGRAM ELEMENT, PROJECT, TASK AREA & WORK UNIT NUMBERS: NRL Problem H02-51, Program Element 61153N, Project RR011 09-41
11. CONTROLLING OFFICE NAME AND ADDRESS: Office of Naval Research, 800 North Quincy Street, Arlington, Virginia 22217	12. REPORT DATE: Dec[redacted]76
	13. NUMBER OF PAGES: 40 p. / 40
14. MONITORING AGENCY NAME & ADDRESS(if different from Controlling Office)	15. SECURITY CLASS. (of this report): UNCLASSIFIED
	15a. DECLASSIFICATION/DOWNGRADING SCHEDULE

16. DISTRIBUTION STATEMENT (of this Report)

Approved for public release; distribution unlimited.

17. DISTRIBUTION STATEMENT (of the abstract entered in Block 20, if different from Report)

18. SUPPLEMENTARY NOTES

This work was sponsored by the Office of Naval Research under Contract RR011-09-41, titled Computational Fluid Dynamics.

19. KEY WORDS (Continue on reverse side if necessary and identify by block number)

Laser fusion
Dynamic stabilization
Rayleigh-Taylor modes
Computational fluid dynamics

20. ABSTRACT (Continue on reverse side if necessary and identify by block number)

By continually modulating the intensity of the driving laser beams, the fastest-growing modes of Rayleigh-Taylor instability on the surface of an imploding laser fusion pellet can be dynamically stabilized. Both theory and numerical simulation are presented to support this conclusion. The band of modes stabilized extends to sufficiently long wavelength that rather high aspect ratio shells apparently can be imploded successfully. Similar beam modulation or bunching techniques should work for electron, ion, and heavy ion pellet implosion schemes.

DD FORM 1 JAN 73 1473 EDITION OF 1 NOV 65 IS OBSOLETE
S/N 0102-014-6601

SECURITY CLASSIFICATION OF THIS PAGE (When Data Entered)

251 950

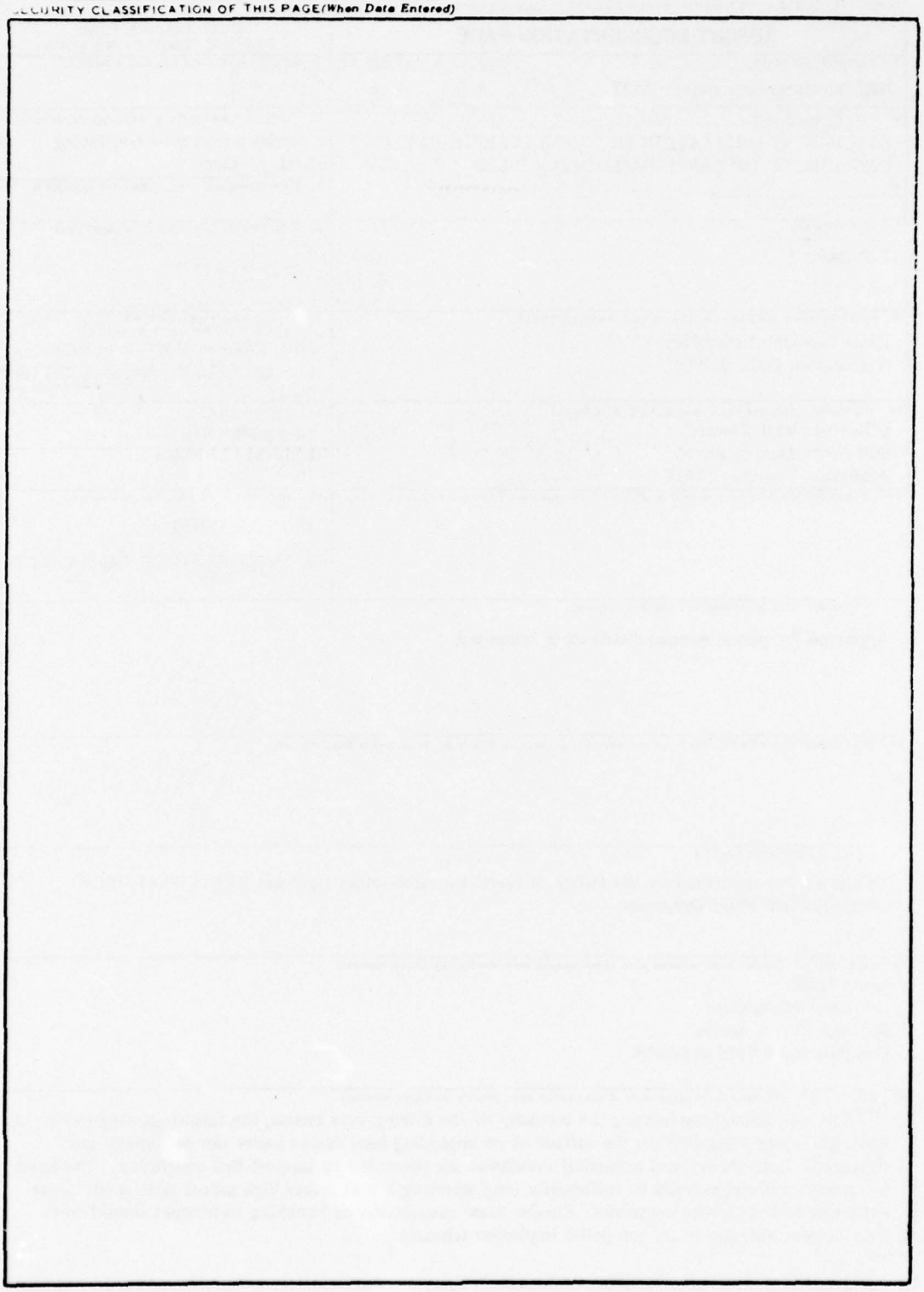

CONTENTS

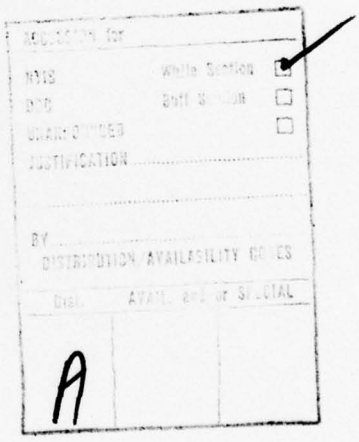

DYNAMIC STABILIZATION OF THE RAYLEIGH-TAYLOR INSTABILITY ON LASER-IMPLODED SHELLS

I. Introduction

In this paper a method for dynamic stabilization of the Rayleigh-Taylor instability on the surface of an imploding fusion pellet is presented and discussed. The technique involves the continual modulation of the driving laser beams so that the potentially Rayleigh-Taylor unstable ablator shell is subject to a rapidly and strongly oscillating acceleration. A band of R-T modes can be stabilized by this oscillation even though the time average acceleration vector lies in the destabilizing direction. By adjusting the frequency, structure, and amplitude of the modulation, the band of dynamically stabilized modes can be made to include the most unstable and dangerous modes. Thus considerably higher aspect ratio shells (i.e., thinner shells) can implode successfully than had been previously considered stable enough.[1] Both theory and fully nonlinear numerical simulations[6] support this conclusion for the case of laser-driven pellet implosions. Similar beam modulation via charged particle bunching should work to stabilize the most dangerous Rayleigh-Taylor modes in relativistic electron beam, ion and heavy ion pellet implosion schemes.

Most schemes for producing thermonuclear fusion by imploding a solid sphere or hollow shell of D-T fuel rely on the symmetry of the implosion to achieve the necessary densities and temperatures at peak compression to initiate the thermonuclear burn process. The prevalent schemes suggested to date (laser beams, electron beams,

Note: Manuscript submitted November 24, 1976.

light or heavy ion beams incident on the surface of a layered pellet) all involve deposition of energy in a thin ablation layer at the surface of the pellet. This energy rapidly heats the dense shell material causing a high pressure region. This pressure maximum drives the shell inward and conserves momentum by accelerating a low density blow-off plasma outward. Since the relatively low density ablation layer is accelerating the higher density shell, the system is unstable to the Rayleigh-Taylor modes which can grow when the acceleration lies parallel to the density gradient.

In the laser-pellet configuration the behavior of the instability is complicated by a host of important physical effects so not even the linear problem has been solved adequately. Computer codes such as LASNEX[2] and FAST2D[3] have been used to study some of the properties of the Rayleigh-Taylor modes via numerical simulation. Although some of the linear properties of the R-T modes have even been uncovered analytically, an accurate dispersion relation including finite sound speed, ablation layer gradients, convection and finite thermal conductivity still does not exist to describe the growth of these modes. Furthermore, the nonlinear growth and turbulence properties are almost entirely a mystery.

Figure 1 shows the density, temperature, and pressure profiles at the outside of a D-T shell being accelerated by electron thermal conduction induced ablation. These profiles are presented exactly as computed by the FAST2D computer code with the laser depositing its energy at the critical layer which lies off the right hand side

of the figure. The $x = 0$ position was chosen to coincide with the peak pressure point so the blow-off lies to the right ($x > 0$) and the accelerating shell lies to the left ($x < 0$). The ablation layer proper extends about 3 or 4 microns from the separation point $x = 0$ out into the blow-off. It results from the strong nonlinear dependence of the thermal conductivity on temperature. A future note will be devoted to a simple two-region quasi-steady-state analytic model of these ablation layers.

Our current attention is directed toward studying the Rayleigh-Taylor instability which occurs in the region from -4μ to 0μ, indicated as Rayleigh-Taylor unstable, where the density and pressure gradients are opposed. The difficulty in performing the linear analysis arises from the fact that the instability develops in an accelerating frame of reference where fluid is convecting through the unstable region at several microns per nanosecond.

II. The Numerical Model

The FAST2D computer code[3] solves the compressible ideal fluid equations in 2D slab geometry with a strongly nonlinear thermal conductivity. Figures 2, 3, and 4 show a developing Rayleigh-Taylor mode in two distinct computer graphics displays. The (a) half of the figures shows contours of mass density at 0.1, 0.2, 0.3, 0.4, and 0.5 gm/cc values. The vertical (y) direction in these plots has periodic boundary conditions and the slab is being accelerated to the left in these figures by the deposition of laser energy at the critical layer $\rho \sim 0.004$ gm/cc near the right hand boundary

of the figure. In the x direction the grid is stretched in the low density regions to the right and left of the slab proper to move the boundaries and their influence as far as possible from the R-T unstable region at the back edge of the shell. The temperature profile at the boundaries and at the critical layer is programmed in ahead of time and provides the mechanism by which the various modulations of acceleration are applied. The fluid has an outflow condition applied at the right and left boundaries.

Figures 2b, 3b, and 4b show the same data plotted perspectively with y increasing to the right and x increasing out of the picture. The density is plotted vertically at three times during the calculation. Figure 2 shows the initial conditions, Figure 3 at .93 nanoseconds shows the instability developing linearly, and Figure 4 at 1.1 nanoseconds shows the characteristic nonlinear development of the compressible Rayleigh-Taylor instability in laser-driven ablations. The nonlinear properties of the R-T modes shown is the subject of future research. The location x(y) of the ρ = 0.1 gm/cc contour shown in the figures is Fourier analyzed to study the spectrum of the surface perturbations and to measure the growth of the Rayleigh-Taylor unstable modes. The two main results of the linear Rayleigh-Taylor analysis using FAST2D are:

1. The long wavelength R-T modes appear to follow the incompressible $\gamma \sim \sqrt{ka}$ law well beyond the wavelengths where sonic communication across a wavelength takes longer than a growth time.

2. There is a cutoff wavelength at which shorter wavelengths are stabilized by the finite thickness of the ablation layer and/or dissipative terms and longer wavelengths grow. The dispersion relation for the modes will be discussed in greater detail in Section III.

The equations being solved in FAST2D are the following:

$$\frac{\partial \rho}{\partial t} = - \frac{\partial}{\partial x}(\rho V_x) - \frac{\partial}{\partial y}(\rho V_y) \tag{1}$$

$$\frac{\partial (\rho V_x)}{\partial t} = - \frac{\partial}{\partial x}(P + \rho V_x V_x) - \frac{\partial}{\partial y}(\rho V_y V_x) \tag{2}$$

$$\frac{\partial (\rho V_y)}{\partial t} = - \frac{\partial}{\partial x}(\rho V_x V_y) - \frac{\partial}{\partial y}(P + \rho V_y V_y) \tag{3}$$

$$\begin{aligned} \frac{\partial E}{\partial t} = & - \frac{\partial}{\partial x}\left[E V_x + P V_x - K_o T^{5/2} \frac{\partial T}{\partial x}\right] \\ & - \frac{\partial}{\partial y}\left[E V_y + P V_y - K_o T^{5/2} \frac{\partial T}{\partial y}\right] \end{aligned} \tag{4}$$

where $K_o \sim 10^{-33}$ is used for D-T and where the temperature has kinetic units of cm^2/sec^2. That is, $P \equiv \rho T$ and $E = \frac{P}{\gamma - 1} + \frac{1}{2}\rho V^2$. The value of γ is taken to be 5/3 throughout the material and the $T^{5/2}$ plasma thermal conduction is used in the shell as well. Splitting algorithms are used along with the latest FCT algorithms[3] to give maximum speed on the Texas Instruments Advanced Scientific Computer at NRL.

The calculations shown in later sections were performed with typical values $0.5\mu \leq \delta x \leq 1.0\mu$, $1.0\mu \leq \delta y < 5\mu$ and with 0.5 picosecond $< \delta t < 2.5$ picoseconds. The sound and flow speeds determine the timestep by the usual Courant conditions and the sliding rezone capability of the FCT algorithms is used to perform the calculation in an accelerating frame of reference which keeps the dense shell material centered in the computation region throughout the run.

Figure 5 shows the temperature profile through the ablation layer as calculated by FAST2D at four different times during a two-dimensional calculation. The solid line shows the profile predicted using a simple two-region steady state theory which inputs the numerical values for upstream density, temperatures, and burn-through rate from the FAST2D calculation. The agreement of the computation with the analysis is very good considering the rather coarse grid resolution at the "singularity". Furthermore, the steadiness of the computed profile in time lends credence to the use of a steady-state theoretical blow-off model even though the ablation layer is only really stationary in an accelerating frame of reference.

III. Analysis of Dynamic Stabilization

The numerical results to date are consistent with a very simple dispersion relation for the growth of the Rayleigh-Taylor modes,

$$\gamma^2 = \frac{ka}{1+k/k_\rho} - \frac{4k^2 a}{3k_\rho} \quad . \tag{5}$$

This has the desired cutoff at $k_c = k_\rho/2$, as supported by simulations, and has $\gamma \sim \sqrt{ka}$ for long wavelength, also supported by simulation. In Eq. (5) the acceleration of the shell is a, k_ρ is the inverse scale length of the ablation layer, and $k = \frac{2\pi}{\lambda}$ is the wave number of the Rayleigh-Taylor modes in the y-direction along the shell. Defining $\epsilon \equiv k/k_\rho$ gives

$$\gamma^2 = k_\rho a \left[\frac{\epsilon}{1+\epsilon} - \frac{4\epsilon^2}{3}\right] \tag{6}$$

where the shortest linearly unstable mode has $\lambda = 4\pi/k_\rho$. Figure 6 depicts this phenomenological dispersion relation, plotting $\gamma/(k_\rho a)$ versus the nondimension wave number ϵ over the linearly unstable range $0 \leq \epsilon \leq 0.5$. Maximum growth occurs at $\epsilon \sim \frac{1}{4}$ (more correctly ~ 0.243) and the value of the growth rate maximum is roughly

$$\gamma_{max} \sim 0.342 \sqrt{k_\rho a}. \tag{7}$$

The first term in Eq. (5) and (6) encompasses the usual simple Rayleigh-Taylor growth without infinite growth at short wavelength. The second term takes the growth to zero but is reactive in this simple form--not dissipative.

In the run shown in Figure 1 and in Figure 5, an estimate of k_ρ can be made. Taking $1.5\mu = 1/k_\rho$ as the scale length for the high density half of the ablation layer, the cutoff wavelength from the

simple dispersion relation is

$$\lambda_c \cong 2\pi \times 2/k_\rho \cong 6\pi\mu, \tag{8}$$

in good agreement with the observation that mode 4 ($\lambda_4 = 25\mu$) grew rapidly but mode 5 ($\lambda_5 = 20\mu$) did not.

To study the effects of modulating the laser beam numerically, I varied the plasma temperature at the critical surface according to a prescribed functional form, constant plus a sinusoidal oscillation. To study the same phenomenon analytically in an illuminating but approximate manner, the dispersion relation Eq. (5) was converted to a second-order ordinary differential equation for the perturbation mode amplitude in which the acceleration term is varied parametrically. This equation,

$$\frac{\partial^2 A}{\partial t^2} = \left[\frac{k_\rho a(t)\epsilon}{1+\epsilon} - \frac{4\epsilon^2 k_\rho}{3} \langle a(t) \rangle \right] A , \tag{9}$$

like the dispersion relation on which it is based, has only a phenomenological/intuitive basis because the linear, time-constant-coefficient problem hasn't been solved satisfactorily to date. The acceleration in the cutoff/dissipation term is taken as a time average although some additional stabilization might result from including in the theory the oscillating thickness of the ablation layer itself.

Let $a(t) = a_o + a_1 \cos \omega t$ where a_o is the time average part and a_1 is the amplitude of the oscillating acceleration. The ordinary differential equation (9) becomes

$$\frac{\partial^2 A}{\partial t^2} = \left[\frac{\epsilon}{1+\epsilon} (k_\rho a_o + k_\rho a_1 \cos \omega t) - \frac{4\epsilon^2 k_\rho}{3} a_o \right] A \qquad (10)$$

where ω is the frequency of the modulation. The time dependence is assumed here to be simple, periodic, and sinusoidal. Later I will discuss pulse shape; there is no reason to assume that the sinusoidal modulation is optimal but at least it is analytically tractable. Identifying with the canonical Mathieu Equation[4] as treated in Morse and Feshbach (see Figure 7) requires $2\phi = \omega t$ and gives

$$\frac{\partial^2 A}{\partial \phi^2} = \left[\frac{4k_\rho a_1 \epsilon}{\omega^2(1+\epsilon)} \cos 2\phi + \frac{4k_\rho \epsilon a_o}{\omega^2(1+\epsilon)} - \frac{16k_\rho \epsilon^2}{3\omega^2} a_o \right] A. \qquad (11)$$

We identify coefficients in the canonical Mathieu Equation,

$$\frac{\partial^2 A}{\partial \phi^2} = \left[\left(\frac{h^2}{2} - b \right) + \frac{h^2}{2} \cos 2\phi \right] A, \qquad (12)$$

$$\text{as} \quad \frac{h^2}{2} = \frac{4k_\rho a_1}{\omega^2} \frac{\epsilon}{1+\epsilon} \quad \text{and} \quad b = \left[\frac{4k_\rho a_1}{\omega^2} \frac{\epsilon}{1+\epsilon} + \frac{16k_\rho \epsilon^2}{3\omega^2} a_o \right]. \qquad (13)$$

Let $f_1 \equiv \frac{4k_\rho a_1}{\omega^2}$ and $\delta \equiv a_o/a_1$. Then

$$\frac{h^2}{2} = \frac{f_1 \epsilon}{1+\epsilon} \quad \text{and} \quad b = \frac{h^2}{2} - \frac{h^2}{2}\delta\left[1 - \frac{4\epsilon}{3}(1+\epsilon)\right] \tag{14}$$

are obtained as the appropriate non-dimensional Mathieu Equation coefficients. Here both a_o and a_1 are positive constants.

With the values of h and b determinable from Eqs. (14) above, we turn to Fig. 7 which shows the stability regions for solutions of Mathieu's Equation. The regions of stability and instability are separated by the solid lines in the figure and we need consider only the upper half plane because h^2 is determined from the physical parameters. Above and to the left of the line labelled b_L at least one of the two independent solutions of Eq. (11) grows without bound. Two stable bands are shown, one between the lines b_L and b_S and the other in the lower right hand corner for large positive b. The first region is accessible by oscillating the laser intensity but the second is not because b is generally less than $h^2/2$. This limit is shown as the dashed line in Fig. 7. For finite values of δ the locus of (b,h) values as a function of ϵ from Eq. (14) is displaced to the left from the dashed line at sufficiently short wavelengths. Under such a displacement only a band of Rayleigh-Taylor modes is stabilized and we need to study the extent of this stable band.

The first stability boundary is given by

$$b_L \approx \frac{h^2}{2} - \frac{h^4}{32} + \frac{7h^8}{1024 \times 32} + \cdots \tag{15}$$

as determined from Abramowitz and Stegun[4]. From the same source the second stability boundary is found to be

$$b_S \approx 1 + \frac{h^2}{4} - \frac{h^4}{128} + \cdots . \tag{16}$$

The subscripts L and S refer to the long and short wavelength limits of the first stable region respectively. We want to find the broadest band of stabilization that can be achieved given some control over ω and a_1 for the modulation.

One needs to determine first the value of f_1 for which the linearly most unstable mode $\epsilon \sim \frac{1}{4}$ lies right on the short wavelength stability boundary. We do this by setting $b(\epsilon = \frac{1}{4}, h) = b_S(h)$ and solving for the value of h^2. The result is relatively simple for small δ(i.e., $a_o/a_1 < \frac{1}{4}$).

$$h_S \approx 4\left[\sqrt{(1-\tfrac{7\delta}{6})^2 + \tfrac{1}{2}} - (1-\tfrac{7\delta}{6})\right]^{\frac{1}{2}} \sim 2. \tag{17}$$

Using $h_S = 2$ in Eq. (14) allows us to determine

$$f_1 = \frac{4k_\rho a_1}{\omega^2} = 10 \tag{18}$$

as the required combination of k_ρ, a_1 and ω such that the linearly most unstable mode is just stabilized by the modulation. Perhaps f_1 can be increased beyond this limit even though a narrow band of short wavelength unstable modes might appear but $f_1 = 10$ is a

simple, easy to remember criterion.

Given δ and f_1, we can solve for the long wavelength limit of the dynamically stabilized band by setting $b = b_L$ and solving for the value ϵ_L at which marginal dynamic stability occurs. We get

$$h^2 - \frac{h^2}{2}\delta\left[1 - \frac{4\epsilon_L}{3}(1 + \epsilon_L)\right] = \frac{h^2}{2} - \frac{h^4}{32} + \cdots$$

which has the approximate solution

$$\epsilon_L \sim \frac{8\delta}{f_1}\left[1 - \frac{8\delta}{f_1}\right]. \tag{19}$$

When $f_1 = 10$, the longest stable wavenumber is

$$\epsilon_L \sim .8\delta\left[1 - \frac{8}{30}\delta\right] \sim \frac{4\delta}{5}. \tag{20}$$

The width of the stabilized band is therefore given by the simple formula

$$\epsilon_L \equiv \frac{k_L}{k_\rho} \approx \frac{4a_o}{5a_1}. \tag{21}$$

Clearly the larger the ratio of a_1 to a_o, the longer the wavelengths that can be dynamically stabilized. In an earlier computer calculation RUN 1G (see next section and Figure 8) the ratio $\delta = a_o/a_1$ was measured to be of the order $\frac{1}{5}$ to $\frac{1}{10}$. It is not clear what to

use as a_1 because of the strong spatial gradients in the region prone to Rayleigh-Taylor instability . Thus $k_L \approx \frac{1}{9} k_\rho$ as an estimate. Since the ablation layer thickness k_ρ^{-1} lay in the range 1μ to 2μ (also estimated by seeking the most unstable wavelength $\lambda_m \sim 13\mu$ and the cutoff wavelength $\lambda_c < 10\mu$), the longest stable wavelength for that run could be expected to lie in the ballpark range of 30μ to $70\ \mu$. In fact the mode with $\lambda = 60\mu$ grew slowly.

To maximize the effectiveness of this dynamic stabilization one clearly wants to minimize ϵ_L in Eq. (20). This is accomplished by reducing δ and increasing f_1 subject to the constraint that short wavelengths "uncovered" at large k by pulling the dynamic stabilization "blanket" to small k (minimizing ϵ_L) do not fracture the shell. There is also another constraint on increasing f_1 which arises because a_1 and ω are really coupled. When ω is too small (to maximize f_1), the value of a_1 also decreases because the ablation layer and the Rayleigh-Taylor unstable region beneath (see Figure 1) can adjust rather quickly to changes in the driving pressure. Assuming that the Rayleigh-Taylor unstable region is oscillated in position according to $\ell \sim \ell_o + \ell_1 \cos \omega t$, the acceleration $a_1 \sim \ell_1 \omega^2$ and is proportional to frequency squared. As ω decreases, at least for small ω, so does a_1. Thus $f_1 \approx 4 k_\rho \ell_1$ is roughly independent of ω, if ℓ_1 is held constant as ω is varied.

Further work is definitely required to pin down more accurately what the accessible regime of values of f_1 is. We turn now to the

very important question of how this dynamic stabilization effect scales with size. Larger pellets with thicker shells implode more slowly so it is correspondingly important to stabilize proportionately longer wavelengths. When the ablating shell thickness ΔR is increased, a_o decreases as ΔR^{-1} since the average shell acceleration goes inversely as the total mass at a fixed pressure. The oscillating acceleration a_1 is unaffected by the shell thickness so the ratio $\delta \equiv a_o/a_1$ also decreases as ΔR^{-1}. This has two advantages when scaling up to larger pellets. First, the long wavelength stable-to-unstable crossover point at $k_L \approx 8\delta k_\rho/f_1$ moves progressively toward longer wavelength (smaller ϵ) as δ approaches zero. This means that longer wavelengths can be stabilized by a given modulation frequency and amplitude in large pellets than in small pellets. Second, a smaller value of δ means that correspondingly lower modulation frequencies can be tolerated since $a_1 > a_o$ is easier to ensure in large pellets than in small.

The conclusion is that, by varying ω, the most unstable mode with wave number $k_m = \frac{1}{4}k_\rho$ can be moved right to the boundary of the stable region near $b \sim 1.8$, $h \sim 1.9$ (or beyond) to maximize the extent of the dynamically stabilized portion of the Rayleigh-Taylor spectrum. Furthermore, as will be seen through complete numerical simulations in the next section, the region actually stabilized is quite broad enough to increase the workable aspect ratio of the imploding shell considerably.

IV. Numerical Simulations of Dynamic Stabilizations

Several sets of computer runs have been performed to test dynamic stabilization in a realistic system which contains the finite sound speed/shock properties of the fluid involved and which also represents accurately in two dimensions the nonlinear thermal conductivity effects expected. The basic code, FAST2D,[3] has been described elsewhere. The calculations are performed on a two-dimensional Cartesian domain with periodic boundary conditions in the y direction. The laser is assumed to be incident from the $x = x_{max}$ boundary of the system and deposits energy at the critical density $\rho \sim 0.004$ gm/cc in such a way that the temperature at the critical density is specified as a controlled time dependent parameter. The location of the critical layer is allowed to change naturally with time and the translation velocity of the coordinate system is chosen so that the dense shell material remains in the center of the region of computation.

Figure 8 summarizes the results of a set of early calculations performed on a 40 x 40 finite difference grid. Three different runs were performed with differing laser intensity profiles. The reference run, labelled RUN 1C, began with a temperature at the critical layer of 1×10^{14} cm^2/sec^2. This corresponds to about 175 ev. The temperature linearly increased to 2×10^{14} cm^2/sec^2 in 0.5 nanosecond and then was held constant at that level for the remainder of the run. The solid curve in the figure shows the velocity of the shell as a function of time up to the point at

which the shell buckled due to the Rayleigh-Taylor instability. There was no laser modulation in the reference calculation and the time of buckling was determined to be that time when the maximum perturbation of the ablation layer was ± 2μ. This, of course, corresponds to a far smaller perturbation of the inside edge of the shell. Figure 3 shows the buckling point pictorially.

The calculation labelled 1B in the figure (x's) was performed using the reference temperature profile plus a 25% oscillation of the laser intensity superimposed. The amplitude of the oscillation therefore was 5×10^{13} cm^2/sec^2 and the oscillation frequency was taken to be three cycles per nanosecond. The shell in RUN 1B accelerated somewhat faster than the reference case 1C because the extra energy deposited at the peak of the oscillation exceeds the energy decrement in the trough of the oscillation because the thermal conductivity is nonlinear. The shell also accelerates for a somewhat longer period of time, reaching a terminal velocity roughly twice the velocity attained in the reference case. The calculation was terminated, not when the shell buckled, but when the laser pulse burned through the ablator material. Thus the shell did not really go Rayleigh-Taylor unstable at the run's termination but rather was simply too thin.

RUN 1G, plotted as triangles in Figure 8, was performed with a 50% oscillation at 2.25 cycles/nsec superimposed on the linear ramp plus constant temperature profile. The oscillating temperature at the critical layer was ± 10^{14} cm^2/sec^2 and the acceleration is correspondingly faster than either the reference case 1C or the

25% oscillation case 1B. The shell again burns through rather than buckling. The velocity attained before burnthrough is now roughly 2.5×10^7 cm/sec and more than six times the kinetic energy per particle has been translated to the shell in the modulated case as opposed to the unmodulated reference case. The time of acceleration and burnthrough for the 50% modulation in RUN 1G is somewhat shorter than the 25% oscillation because the rate of acceleration and ablation of material is somewhat larger.

In the reference case 1C the linear growth rates for the modes near the peak of Figure 6 could be determined roughly from the calculation and supported at least semi-quantitatively the dispersion relation of Eq. (5). Detailed linear numerics is very difficult to perform and analyze because the "equilibrium" is constantly changing in time and because the propagation of large amplitude compressional and sound waves through the shell clearly affects the Rayleigh-Taylor growth strongly. Sound waves, for example, can locally reverse the density gradients and temporarily stabilize the Rayleigh-Taylor modes over half a cycle. Of course, the modes are presumably more unstable in the second-half cycle of a sound wave when the gradients become steeper but there is no reason to expect the phenomena to cancel on average. The finite amplitude sound waves also effectively transmit perturbations at the outer edge of the shell throughout the shell volume during the initial ramp-up phase.

To pursue dynamic stabilization further, runs with a thicker shell were clearly required

and runs with $\delta y > \delta x$ were needed to study the effects of dynamic stabilization on longer wavelengths. Greater resolution was also called for to increase the breadth of the potentially unstable portion of the spectrum. A set of two calculations called DUMP2A were performed on an 80 x 80 finite difference grid with a somewhat higher base temperature and with a shell thickness of 37μ initially. The idea was to perform an entire reference calculation without modulation and then to restart that identical calculation in the middle when initial wave amplitudes had grown out of the early random noise and mode growth was beginning to occur in an organized linear manner. The modulated case was restarted with a 33% oscillation at two cycles/nsec and the evolution of the same initial conditions with and without modulation is compared. The driving temperature ramped linearly up to 3×10^{14} cm^2/sec^2 and then was held constant for the duration of the reference calculation. The amplitude of the oscillation added to this constant temperature was 1×10^{14} cm^2/sec^2. Earlier Figures 1 and 5 showed the ablation layer details and theoretical computations for the ablation layer structure for the DUMP2A run. The data in Figure 9 are plotted for Modes 1, 2, and 4 with wavelengths of 100μ, 50μ, and 25μ, respectively. From about 3.25 nsec,on roughly exponential growth can be seen for these three modes in the reference case. The problem was initialized with modes 4 and 8 excited.

At 3.25 nsec the mode structure was sufficiently well developed and yet the amplitudes were sufficiently small that the modulation

could be started and the dynamic stabilization properties of this modulation could be tested in a difficult case which had been allowed to grow linearly for more than 3 nsec. The two data curves shown in Figure 9 apply to modes 2 and 4 and demonstrate that the amplitude of the ablation layer perturbations became essentially oscillatory and stopped growing at a couple tenths of a micron amplitude. In the reference calculation the shell became Rayleigh-Taylor unstable and broke at about 6-6.5 nsec. The two micron perturbation limit was again used as a signature of shell breaking for the unmodulated reference case and the modulated case showed shell burnthrough rather than Rayleigh-Taylor buckling (Fig. 3,4).

It is important to note that often times the longest wavelength in the system acquires appreciable energy because the system computed does not provide a continuum of modes near the longest mode. In DUMP2A, for example, the unmodulated case showed mode 1 almost as large as mode 2 and mode 4 even though the linear growth of mode 1 should be the slowest of the three (or at least slower than mode 2). The only solution to this problem of k-space discreteness/blocking is to use finer grids and larger systems.

Figures 10 and 11 summarize results from two runs performed to study the long wavelength effects in a system with the thicker 37μ shell. These cases, RUN 2B and RUN 2C, used the same reference temperature profile as DUMP2A but the temperature oscillation amplitude was increased to 50% as shown in Figure 10a. The period of the oscillation was reduced to 1 cycle/nanosecond to maximize f_1

and hence to broaden the band of dynamic stabilization as much as possible commensurate with keeping the shell entirely within the region of computation. Figure 11a summarizes the average shell velocity history for these runs which differed only in the value of δy ($\delta y = 1.25\mu$ for RUN 2B and $\delta y = 3.75\mu$ for RUN 2C).

Again the shell burned through rather than breaking due to Rayleigh-Taylor instability. The shell attained a velocity of 3.5×10^7 cm/sec and showed no serious buckling before burnthrough. The outer surface perturbations for the two runs for the three longest wavelength modes are plotted in Figures 10b and 11b. In both cases the dashed line shows the linear growth pattern expected according to Eq. (5) for the longest wavelength in the system (slowest growth). In both RUN 2B and in RUN 2C the mode growth falls far below the linear growth lines even though two out of the three modes plotted should grow much faster. In both cases the outer surface perturbation at burnthrough was at most a couple tenths of a micron, a good order of magnitude <u>below</u> the level used to signal Rayleigh-Taylor buckling in reference calculations such as shown in Figure 3.

Figure 11b shows that modes of at least 300μ wavelength along the shell are dynamically stabilized by modulating the laser intensity. Using a time of 6nsec and a speed of 3×10^7 cm/sec gives an average acceleration of $a_o \sim 5 \times 10^{15}$ cm/sec^2 for the run. The fluctuating acceleration also shows in Figure 11a and is 2-4 times the average. Thus $a_1 \sim 1 - 2 \times 10^{16}$ cm/sec^2. Plugging into

Eq. (18) defining f_1 and using $k_\rho^{-1} \sim 1.5\mu$ and $\omega = 2\pi \times 10^9$ sec^{-1} gives $f_1 \sim 7$ - 13 which nicely brackets the theoretical target value of $f_1 \sim 10$.

In 6 nsec at an average velocity of roughly 1.5×10^7 cm/sec the shell travels 900μ. If the initial spherical shell were of order 1000μ in radius, this case would represent a (relatively) successful implosion of a 30 : 1 aspect ratio system.

V. Conclusions

The theory and calculations presented in this paper support the conclusion that an appreciable band of the unstable Rayleigh-Taylor spectrum on the surface of an imploding laser pellet can be stabilized by modulating the intensity of the driving laser beams. By just stabilizing the linearly most unstable mode, the band of complete stabilization can be extended to modes with wavelengths more than ten times the shell thickness. The growth of slower long wavelength modes is not stabilized by the modulation but the implosion time is sufficiently short that these residual modes should not have time to seriously distort the shell before implosion occurs.

The crucial question of how large the constant f_1 in Eq. (18) can be made and hence how broad a band of modes can be stabilized is at best partially answered. In one of the early 40 x 40 calculations a frequency of 6 cycles/nsec was tried and the shell went Rayleigh-Taylor unstable almost as if no modulation had been applied. A high frequency cutoff like this is expected because temperature oscillations at the critical layer can't be felt at the ablation layer unless

their period is longer than the heat diffusion time.

A 40 x 40 run was also performed with a modulation frequency of 1 cycle/nsec but this proved to be too long on such a small system. In the troughs of the oscillation the shell tried to expand out of the computation region, a problem later rectified in a series of 80 x 80 calculations. For the typical parameters of interest here frequencies of ~ 0.5 cycle/nsec and slower have yet to be considered and may work best of all. Clearly, however, the period of the modulation can't be longer than a few growth times. It may even be possible to leave short wavelength modes unstable to stabilize even longer modes. Certainly the range of interesting ω values spans about an order of magnitude.

Dynamic stabilization works in the laser-driven implosion because the shell must compress somewhat to transmit the acceleration from the ablation layer on the outside throughout the shell. Therefore an outward acceleration is necessary to relieve the shell compression when the laser intensity reaches a minimum. The fluid compressibility acts as a spring so that the fluid acceleration seen in the Rayleigh-Taylor unstable region actually changes sign even though the laser beam pushes the shell only inward. For dynamic stabilization to work, an average destabilizing acceleration must at least change sign and the oscillating component must exceed appreciably the constant component in amplitude.

The theory was performed using the Mathieu Equation which in

turn assumes a sinusoidal variation of the acceleration. Work is currently underway to provide a numerical capability for integrating the time dependent mode amplitude equations for a spectrum of Rayleigh-Taylor modes from $k = k_\rho$ to $k = 0.01k_\rho$. Then an approximate evaluation of the relative efficiency of various non-sinusoidal acceleration profiles can be carried out rather quickly. A good 1D piggyback code would have to be used to study in detail the exact amount of stabilization provided by laser modulation with any given profile.

Since the portion of the laser energy which gets deposited at the critical surface depends on a number of laser and fluid parameters and since the thermal conduction, which converts temperature at the critical layer to acceleration at the ablation layer, is highly nonlinear, one can only guess what the laser intensity profile would have to be in order for the acceleration to be sinusoidal as assumed in the theory. It is safe to guess that the numerical simulations performed to date are not yet optimum and, therefore, the stabilization conclusions presented are correspondingly conservative. What also remains to be determined is the effect on dynamic stabilization of the host of non-ideal effects such as radiation, atomic physics, realistic equations of state, self-magnetic fields, and supra-thermal particle effects which can also broaden the ablation layer and hence change the short wavelength cutoff.

In pellet fusion schemes where the implosion requires electron,

ion or heavy ion beams to provide the energy required at the pellet surface, the ablation layer, and potentially R-T unstable region beneath, nevertheless acts as a spring storing up compressional energy. If the impinging particle beam were interrupted or reduced in intensity, the stored compressional energy is again available to provide a reverse acceleration just as in the case of a modulated laser. Thus dynamic stabilization is potentially useful for these charged particle beam fusion schemes as well. A shaped cavity could be used to modulate relativistic electron beams[5] and similar electromagnetic or magnetic techniques during the formation, acceleration and transport of ion beams might readily be employed. In all these cases, based on our laser-DT shell calculations, modulation frequencies of a few tenths to a few cycles per nanosecond seem to be required. This would demand particle bunches from a few inches to a few feet in length. For large charged-particle-driven systems one might expect modulations even slower than one cycle per nanosecond to be effective because the sonic response time of a thicker ablation layer would be correspondingly slower. It is this ablation layer response which determines the oscillating component of the acceleration and hence the width of the dynamically stabilized band of Rayleigh-Taylor modes.

Acknowledgments

The author wishes to thank Steve Bodner and Wally Manheimer for many useful discussions, for help, and for graciously submitting to intermittent brain-picking. The author also wishes to thank Professor J. A. Wheeler for demonstrating dynamic stabilization of an inverted pendulum in a Freshman physics lecture many years ago. This work was supported by the Office of Naval Research.

References

1. R. E. Kidder, Nuclear Fusion 16 (1), 1976.
2. G. Zimmerman, Lawrence Livermore Laboratory Report U.C.R.L - 74811, also J. D. Lindl, and W. C. Mead, Lawrence Livermore Laboratory Report U.C.R.L. - 77041, Oct. 1975.
3. J. Boris, Proceedings of the Second European Conference on Computational Physics, Garching, 27-30 April 1976. published by North-Holland. For basic algorithms and splitting techniques see J. P. Boris and D. L. Book, Chapter 3, Methods in Computational Physics, Vol. 16, (Academic Press, New York, 1976) and J. P. Boris, U. S. Naval Research Laboratory Memorandum Report 3237, March 1976.
4. M. Abramowitz and I. Stegun, Eds., Handbook of Mathematical Functions, AMS-55, GPO-June 1964. Also P. M. Morse and H. Feshbach, Methods of Theoretical Physics, Vol. I, Chapter 5, (McGraw-Hill, New York, 1953).
5. M. Friedman (private communication)
6. J. P. Boris, "Dynamic Stabilization of the Imploding-Shell Rayleigh-Taylor Instability," Comments on Plasma Physics and Controlled Nuclear Fusion, to be published.

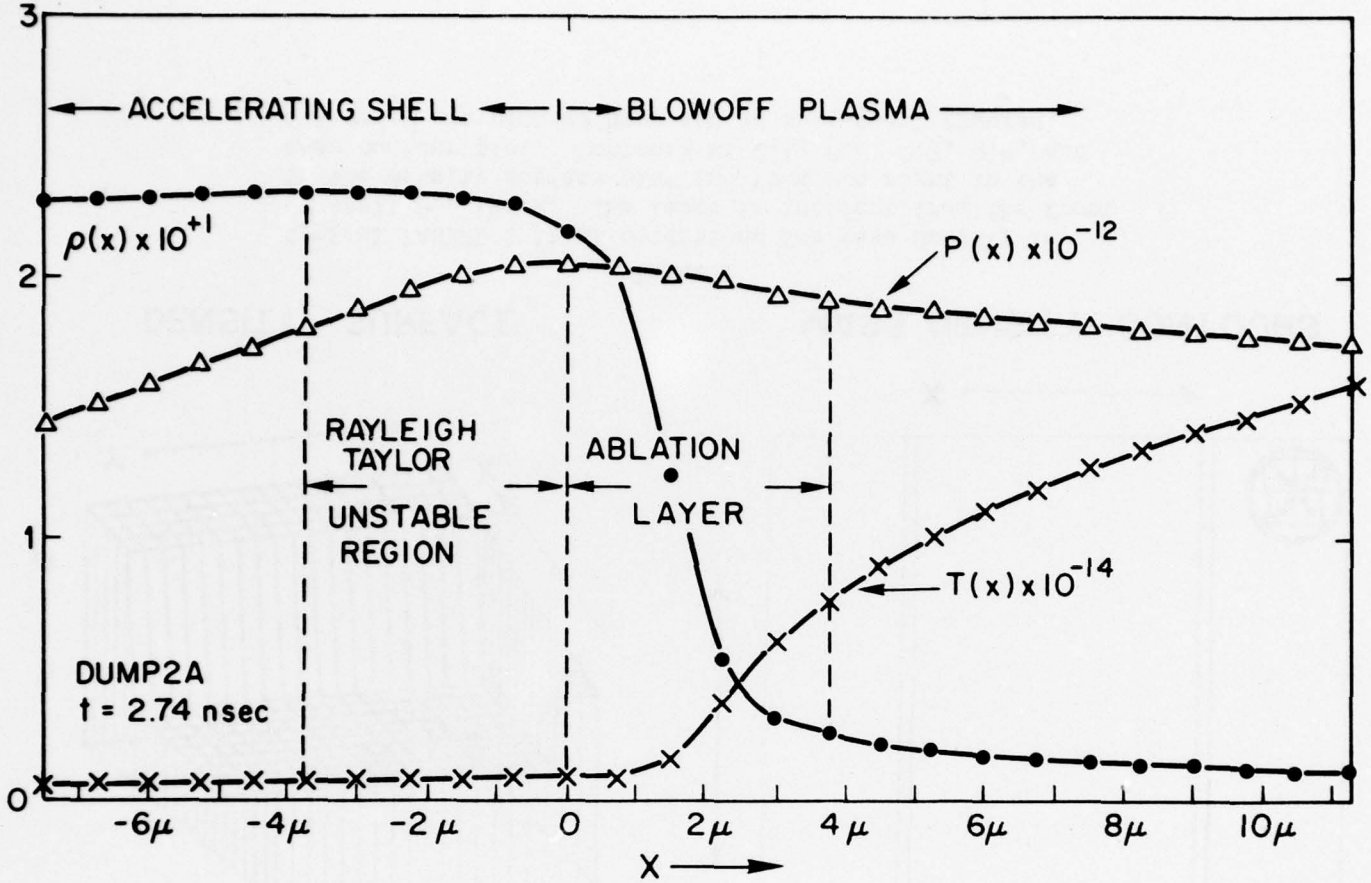

Figure 1

Density (•), pressure (Δ) and temperature (x) profiles for a thermal conductivity ablation layer. Data are taken from a two-dimensional simulation using FAST2D. The temperature at the critical layer was taken to be 3×10^{14} cm^2/sec^2 (about 500ev). The Rayleigh-Taylor modes are potentially unstable where density and temperature gradients are opposed.

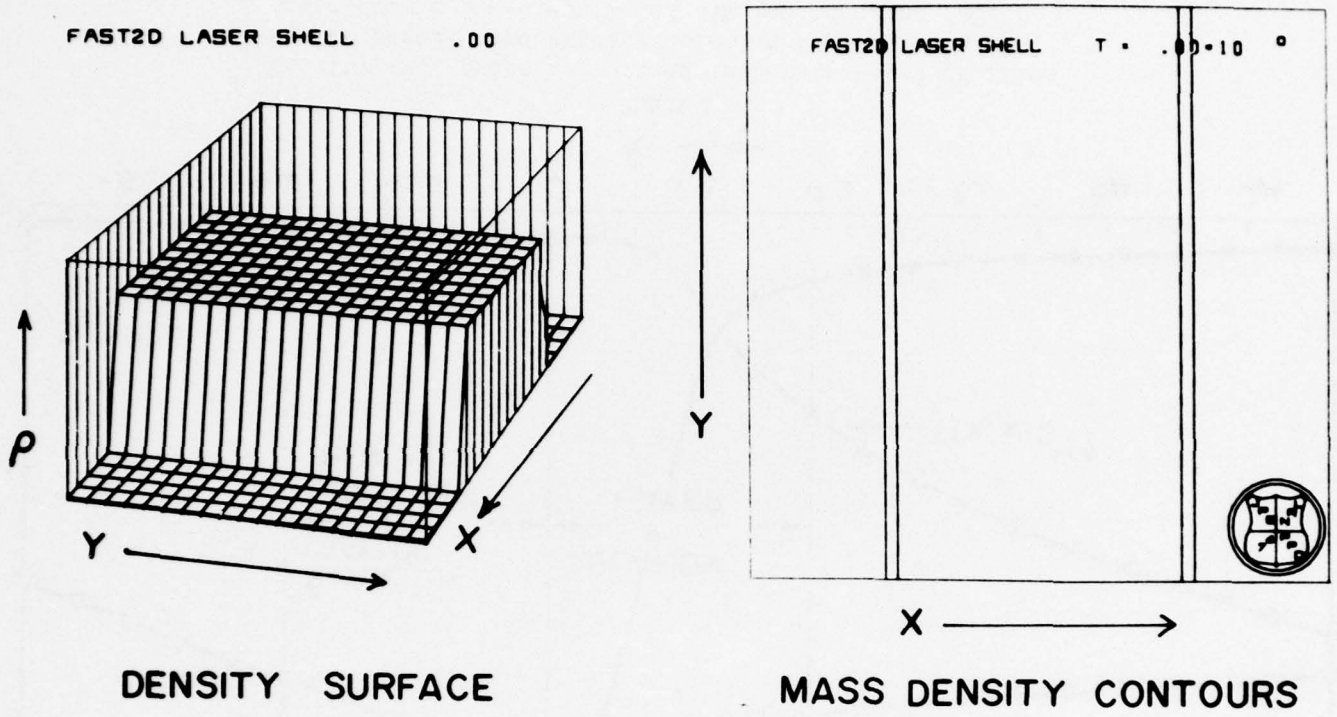

Figure 2

Typical FAST2D initial conditions for mass density in DT shell 20μ thick. The laser is incident from the front in the density surface plot and from the right in the mass contour plot. Contours at 0.1, 0.2, 0.3, 0.4, and 0.5 gm/cc are plotted here and in subsequent figures.

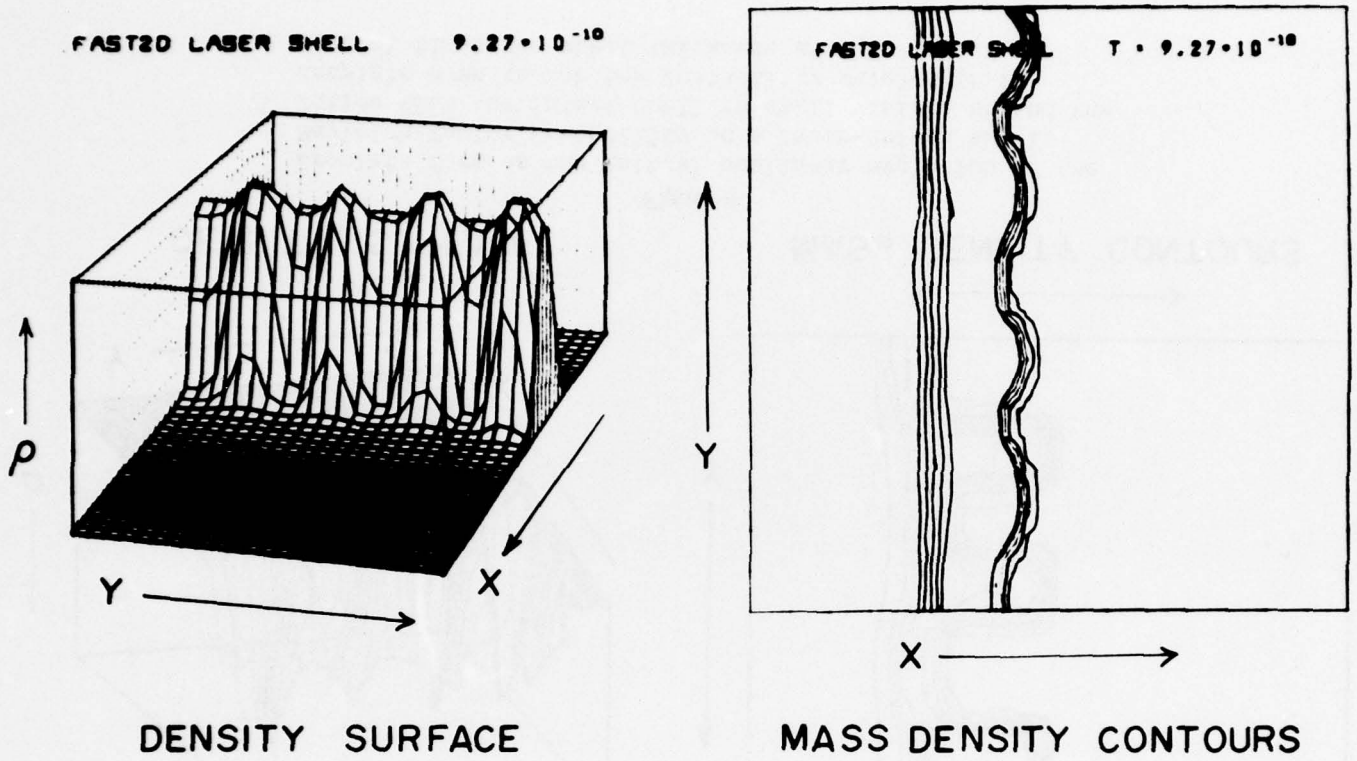

Figure 3

Rayleigh-Taylor buckling of DT shell initially 20μ thick. Notice that the shell has compressed due to the driving pressure. This amplitude of perturbation is used to signal shell failure, about 2μ in the largest harmonic on the outside of the shell. The perturbation of the inner surface is much less.

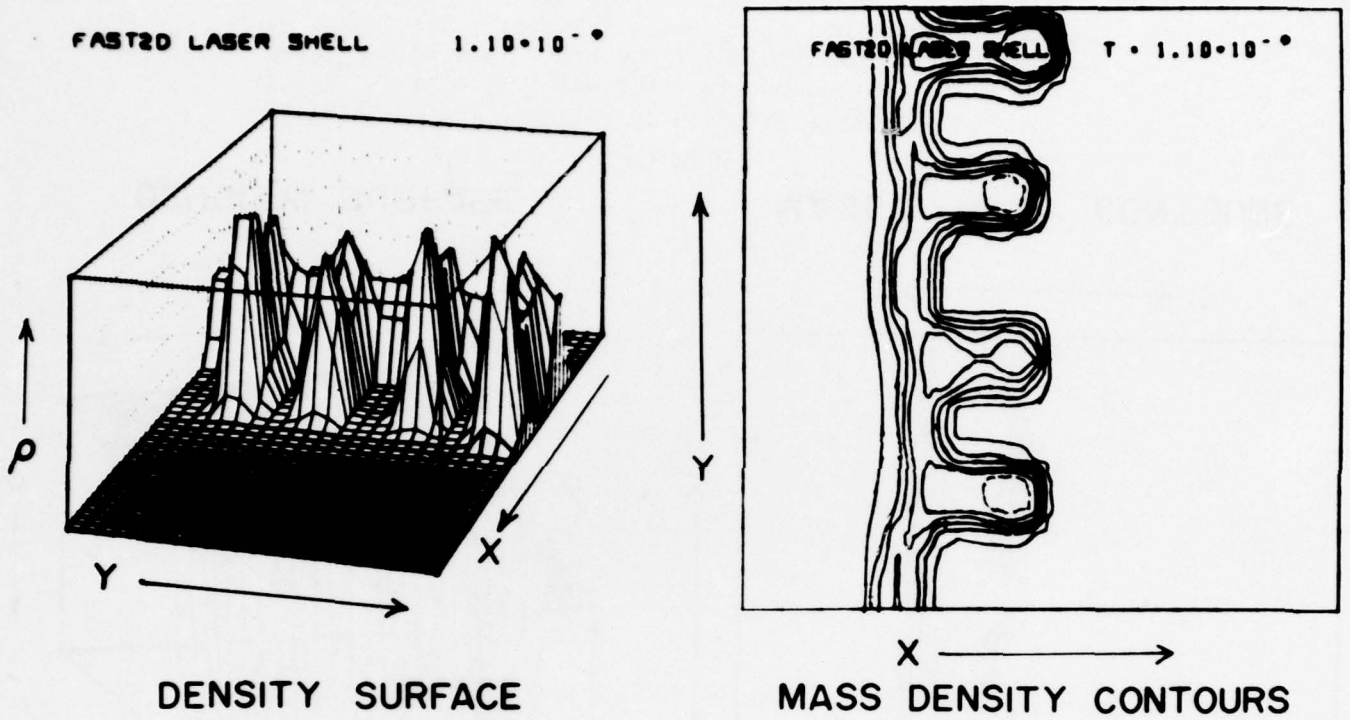

Figure 4

Droplets form as the natural nonlinear evolution of the Rayleigh-Taylor instability on a laser-driven shell. Notice that the intact shell is still visible behind the droplets even though the instability wavelength is several times the shell thickness at this time.

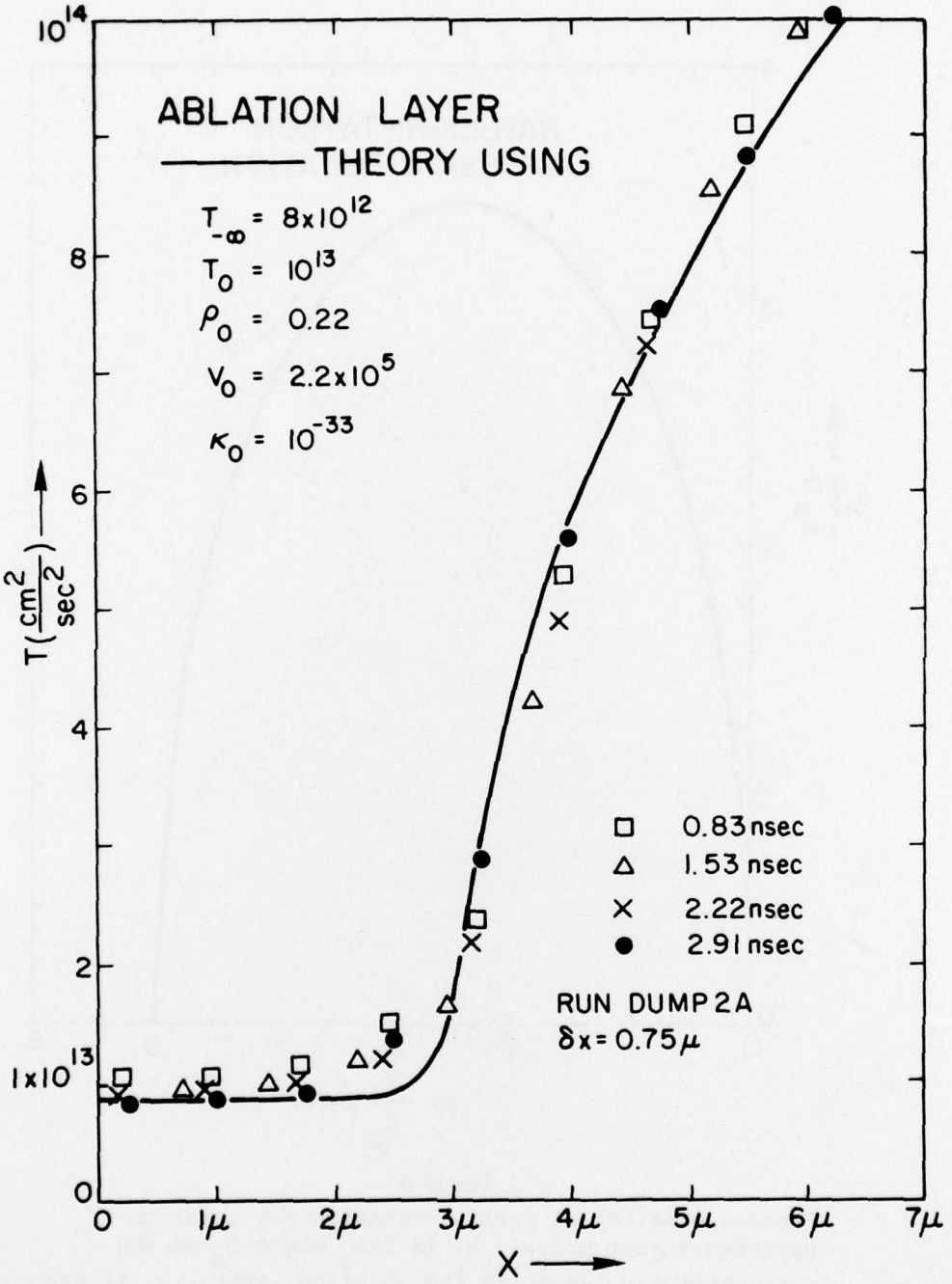

Figure 5

Comparison of ablation layer structure computed by FAST2D (data points) with a simple two-region analytic model (solid curve). The analytic model solves the three time independent conservation equations to the right of the inflection point and the time independent constant density thermal conduction problem to the left.

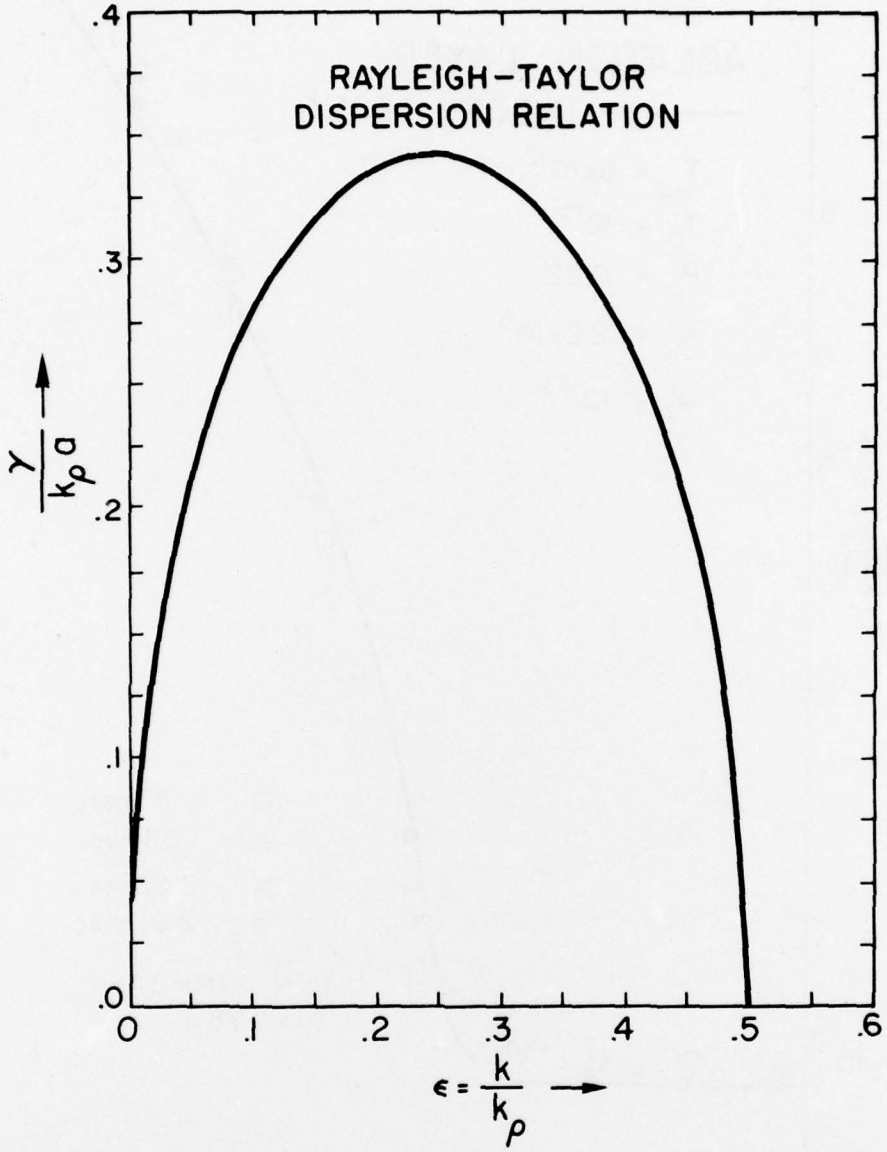

Figure 6

Phenomenological dispersion relation for ablation Rayleigh-Taylor modes. k_ρ is $1/L_\rho$ where L_ρ is the characteristic length in the ablation layer. a is the acceleration and γ the mode growth rate. Long wavelength growth rates are $\sqrt{ka}$ and the short wavelengths stabilize due to the cutoff at $k = k_\rho/2$. Maximum growth occurs at $k \approx k_\rho/4$ and is about one-third of the simple $\sqrt{ka}$ value.

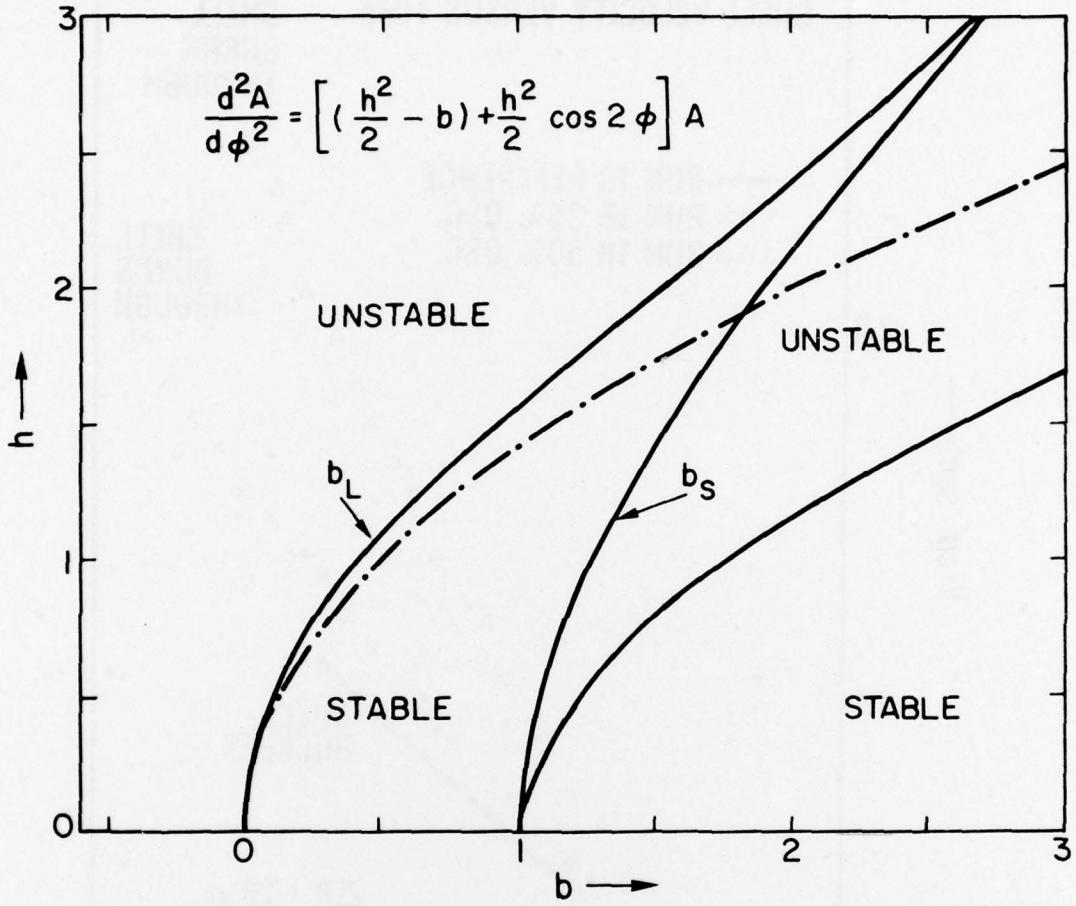

Figure 7

Stability diagram for the Mathieu Equation. The region of b-h parameter space between the curves labelled b_L and b_S is dynamically stabilized by the oscillatory modulation. The dashed curve is the locus of the Rayleigh-Taylor spectrum in the limit of large amplitude oscillations. The locus displaces to the left slightly as the average acceleration approaches the size of the oscillating component.

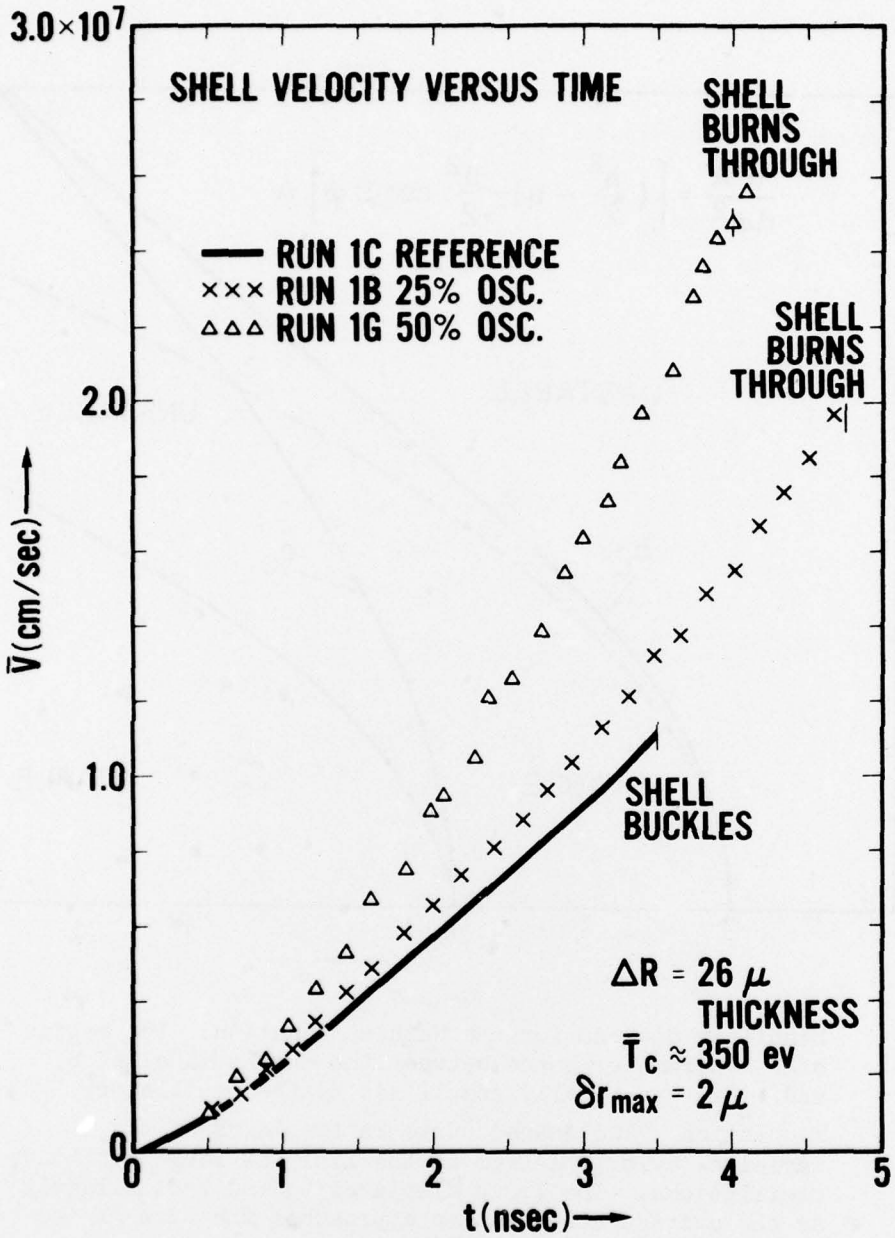

Figure 8

Comparison of shell velocity versus time trajectories for three calculations demonstrating dynamic stabilization of the laser shell Rayleigh-Taylor mode. With dynamic stabilization the shell does not buckle due to the Rayleigh-Taylor instability before the ablator material simply burns through.

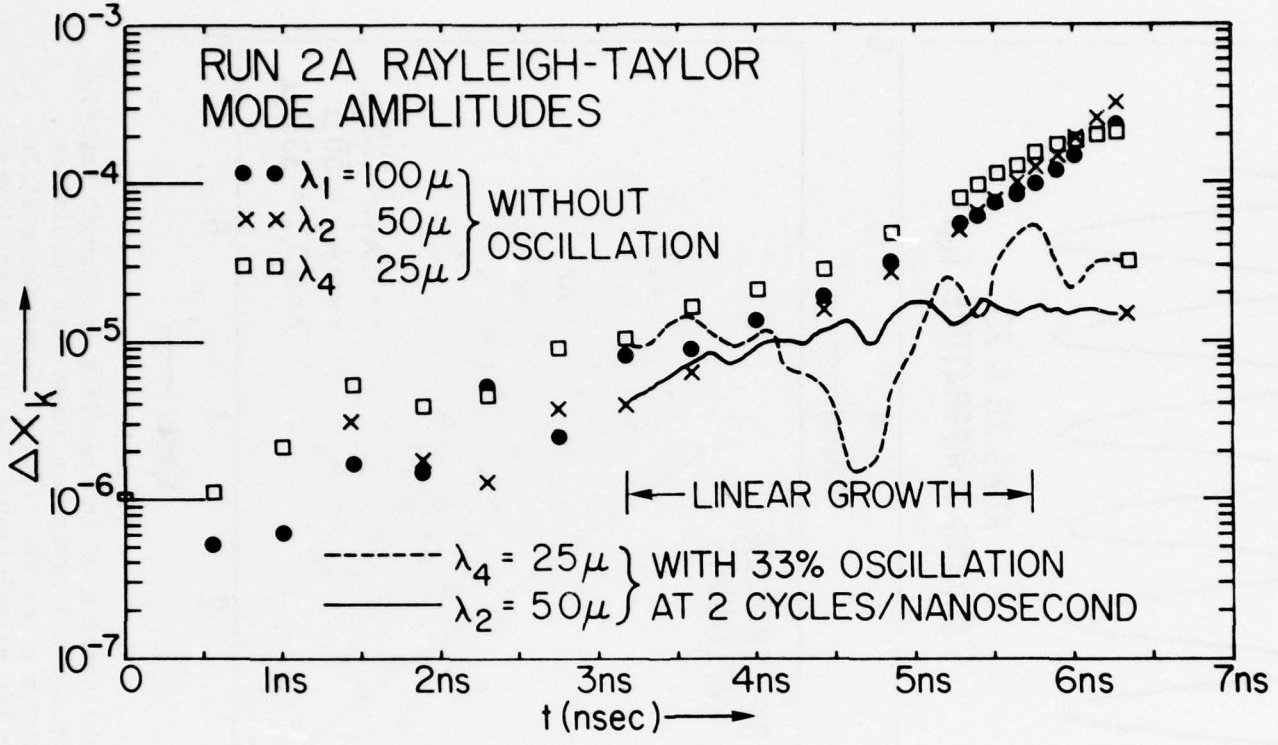

Figure 9

Comparison runs with and without 2 cycle/nanosecond modulation of laser. Even turning modulation on after linear growth has established does not prevent dynamic stabilization of the R-T mode.

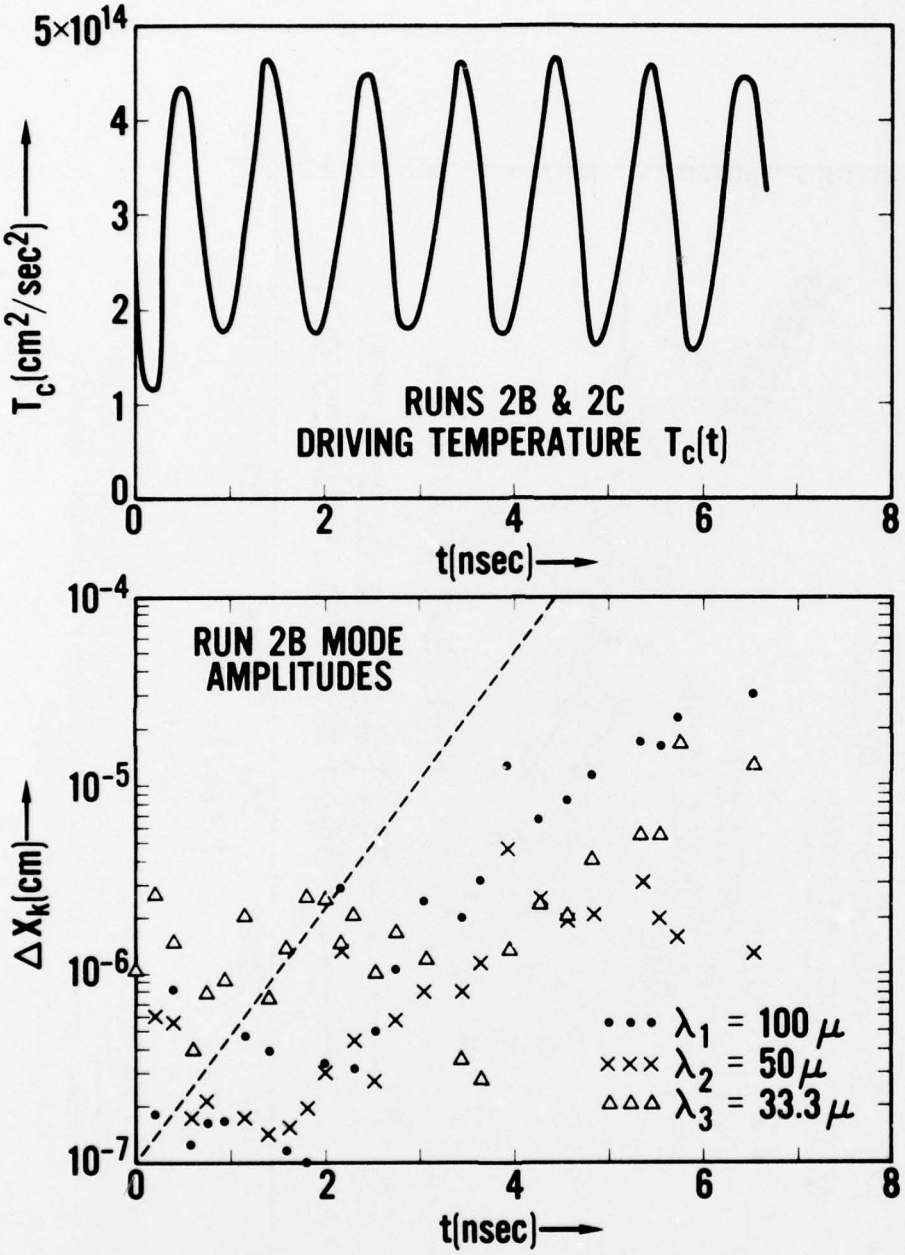

Figure 10

Dynamic stabilization of intermediate wavelength Rayleigh-Taylor modes for a 1 cycle per nanosecond modulation. The upper curve gives the critical layer temperature history for the calculation. The data in the lower figure show the mode amplitude time histories for three wavelengths in the system. The dashed line shows exponential growth at the unmodulated growth rate of the $\lambda_1 = 100\mu$ mode.

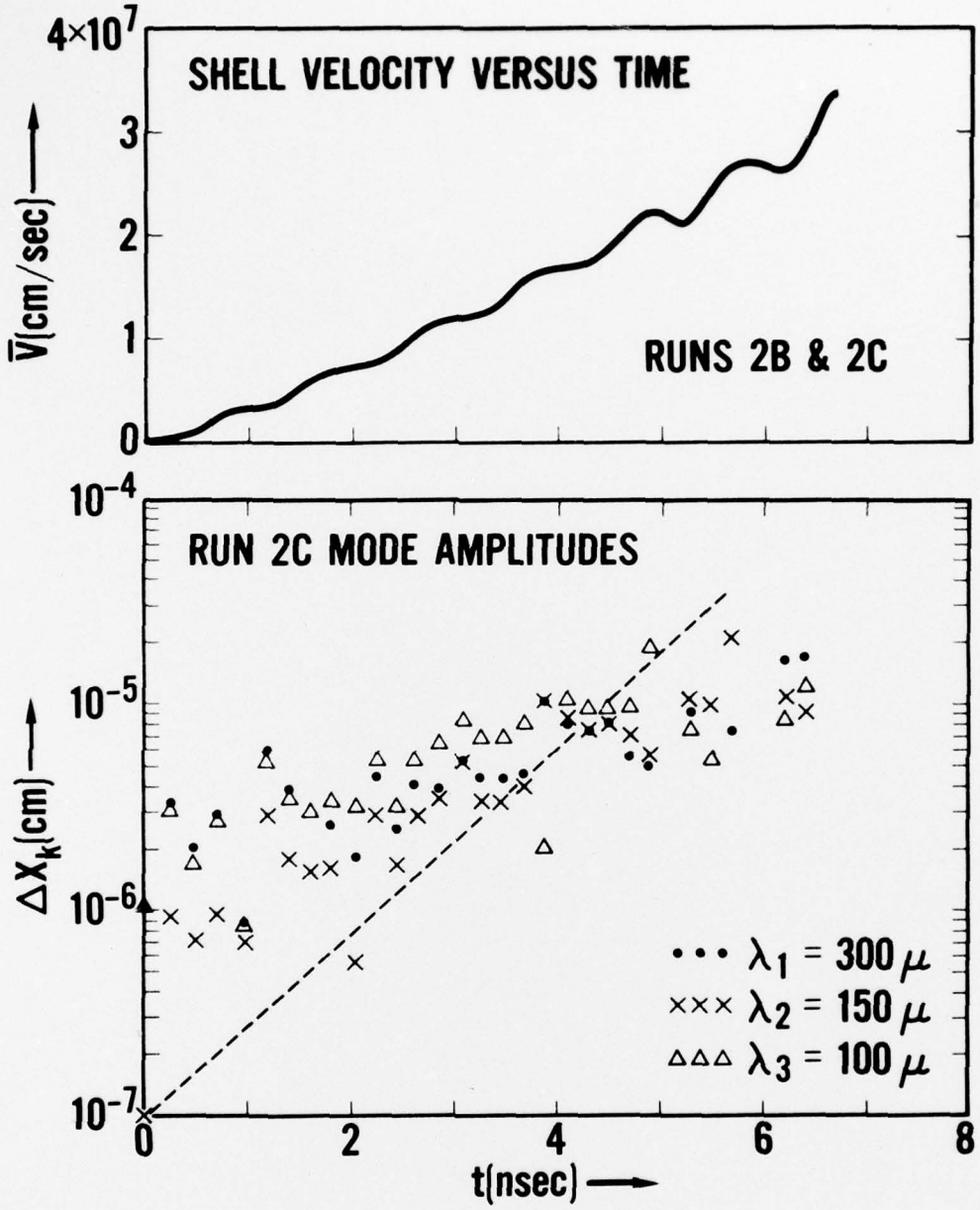

Figure 11

Dynamic stabilization of long wavelength Rayleigh-Taylor modes for a 1 cycle per nanosecond modulation. The upper curve gives the average shell velocity versus time trajectory for the runs 2B and 2C. 3.5×10^7 cm/sec was achieved without instability of the normal R-T type. The three wavelengths in the lower figure all lie below the dashed line, the linear growth line for the $\lambda_1 = 300\mu$ mode. Note that, on burnthrough, the outer surface perturbation is still only 0.1-0.2μ.